

Plume diagnostics of an applied field arcjet by using a diode-laser absorption technique

Kimiya Komurasaki, Teruhito Iida, Daisuke Kusamoto, FengYuan Zhang
 Department of Aerospace Engineering, Nagoya University
 Furo-cho, Chikusa, Nagoya 464-01, Japan
 and
 Shin Satori
 The Institute of Space and Astronautical Science
 Yoshinodai, Sagami-hara 229, Japan

Abstract

Diode-laser absorption spectroscopy technique was applied to the measurement of arcjet plume properties, such as flow velocity, density and temperature. The flow velocity was derived from the Doppler shift of an absorption line of oblique laser probes, and the temperature was from the Doppler broadening of the absorption line. Two-dimensional plume profiles were obtained by coupling the laser absorption diagnostics with the computer tomography method. Finally, swirl velocity caused by applied magnetic fields was measured with a perpendicular probe laser to the plume.

Nomenclature

B : magnetic induction
 c : speed of light
 e : electronic charge
 f : transition oscillation strength
 I_p : transmitted laser intensity through a Fabry-Perot etalon
 I_t : transmitted laser intensity through an discharge tube
 I_0 : incident laser intensity
 I_ϕ : transmitted laser intensity through a plume
 k : Boltzmann constant
 M : mass of an argon atom
 m : electronic mass
 N : number density of neutral particles
 r : distance from the thruster centerline
 r_{arc} : arc attachment radius on the diverging part of anode
 T : translational temperature of neutral particles
 V : local flow velocity of a plume
 x : axial position from the exit plane
 ϕ : incident angle of a laser beam
 κ : absorption coefficient
 κ_0 : κ at the absorption-line center frequency
 ν : frequency

ν_0 : absorption-line center frequency
 ν_D : Doppler shift
 $\Delta \nu_0$: Doppler half width
 $g_D(\nu)$: Doppler line shape function

Introduction

An arcjet thruster is a useful propulsion device for both near-earth transportation and interplanetary missions because of its high specific impulse and high thrust density. However, the specific impulse of arcjets is higher than that of chemical propulsions by only few hundred seconds, and the superiority might be canceled when the weight of power units is taken into account. Since the specific impulse is a function of the stagnation temperature of the arc-heated propellant gas, plasma confinement from the electrodes by means of an applied magnetic field is one of the methods to increase the specific impulse.

Furthermore, the electromagnetic forces produced by the interaction between discharge current and the applied magnetic field (swirl acceleration) is another possibility to increase the specific impulse. The plasma starts to rotate in the azimuthal direction in the arc-discharge region by Lorenz force, and the rotation momentum is converted to thrust through the solid nozzle.

On such plasma confinement or swirl acceleration, direct measurement of the arcjet plume^{1,2)} will bring us valuable information, though it is quite difficult due to the plasma enthalpy and its speed.

Spectroscopic measurement is a promising technique for arcjet plume diagnosis, because it enables us to know the profiles of local flow velocity, temperature and density simultaneously without any direct access into the plasma flow. Although the laser induced fluorescence (LIF) spectroscopy is an established diagnosis methods applicable to the high enthalpy and high speed flows,^{3,4)} recent progresses in semiconductor diode lasers makes the diode-laser spectroscopy in use in both pure and applied spectroscopy, because they are compact, rapid, cost effective, simple to operate, and compatible with optical

fiber transmissions.⁵⁻⁹⁾

The wavelength of the diode-laser beam is easily tunable in the range of 660-1550 nm by controlling the diode working temperature and injection current. Scanning rate of the wavelength can be up to the order of kHz. Meanwhile, the capability to focus the probe laser into the specific location allows the measurement with high spatial resolution.

The objective of our research is to apply the diode laser spectroscopy technique to the arcjet plume diagnosis for the improvement of the thruster performance.

Experimental Apparatus

Arcjet Thruster

A 4-kW class arcjet thruster with an applied magnetic field was made and tested at the Nagoya university. Figure 1 shows a schematic diagram of the arcjet thruster. It consists of a thoriated tungsten cathode, a water cooled copper anode and a ceramic solid nozzle. The cathode diameter and tip angle are 5.0 mm and 30 degrees, respectively. The anode has a 3.0 mm long and 2.0 mm diameter constrictor channel. The nozzle divergent angle is 25 degrees and the exit plane diameter is 52 mm. Magnetic fields are induced by a solenoidal coil circuit independent of the main discharge. Maximum magnetic induction is 0.08 T on the thruster centerline.

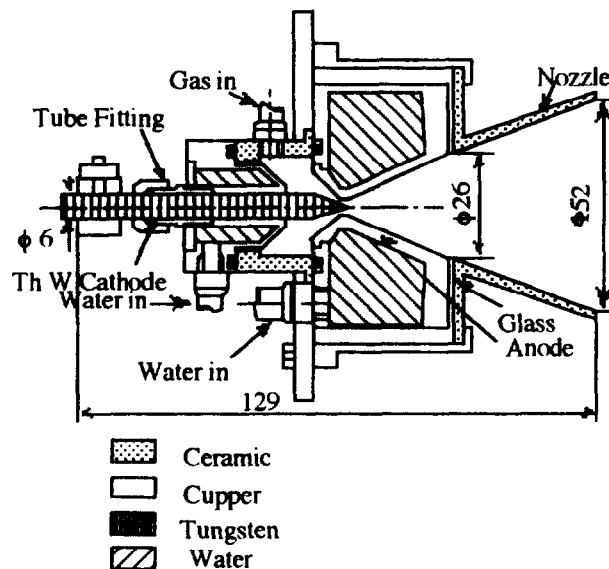


Fig. 1 A cross section view of the arcjet thruster

The arcjet thruster is installed in a vacuum chamber of 1.2 m in diameter and 1.5 m long. It is evacuated by a pumping system consisting of two diffusion pumps, a

roots blower, and a rotary pump. The total pumping speed is 10,000 l/sec and the background pressure has been maintained under 0.3 Torr during the arcjet operation. The propellant mass flow rate is regulated using a thermal mass-flow controller.

Thrust is measured using a thrust stand with a load cell. Calibration is conducted with a pulley and weight system under the vacuum condition. Mean flow velocity at the arcjet exit plane can be derived from the measured thrust and the propellant mass-flow rate.

Diode laser absorption diagnosis

Optic system

Figure 2 shows the diode laser absorption spectroscopy system. A diode LT017MDO (SHARP Corp.) is used as a laser source. It is attached to a copper block for keeping in thermal contact with a temperature controller consisting of a film heater, a Berthier cooler and a sensing thermistor. A collimating lens is set on an adjustable block in front of the diode.

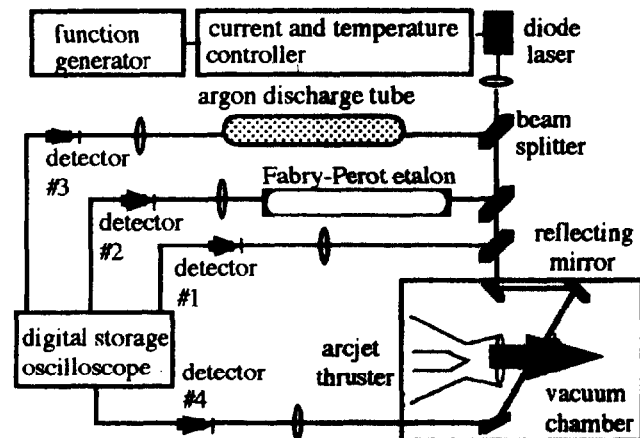


Fig. 2 Schematic of the diode laser absorption spectroscopy system.

An active electronic feedback control is done by an LD driver (ALP-7033CA, ASAHI Data system Corp.) to stabilize the laser power and laser oscillation frequency. The diode temperature fluctuation has been kept within 0.01K. The tunable wavelength is from 790 nm to 830 nm with our setup. The diode laser nominally provides an output power of 40 mW/cm² at a wavelength of 810 nm with a driving current of 65 mA at 25.0 C. It is driven by a low noise current source modulated with a sub-audio function generator.

Output of the diode laser is split into four components.

The first component is directly recorded with a photo-diode detector #1 as a function of time. The second passes through an argon discharge tube, in which steady discharge is maintained in a microwave cavity. The transmission signal is detected by #2 to give the reference peak frequency of absorption line. The third component passes through a Fabry-Perot (FP) etalon, and detected by #3 to provide a reference wavelength spacing during the scanning of laser-oscillation frequency. The data are used as a gauge to convert the temporal absorption variation to the function of frequency. Rest of the laser beam passes through the argon plume exhausted from the arcjet. The signal is recorded by detector #4.

The laser was modulated with a triangle-shape injection current at a rate of 50 Hz superimposed on a dc 70 mA. Keeping the diode temperature at 23.30 C, laser wavelength was scanned from 810.50 nm to 812.06 nm around the center wavelength of Ar I absorption line of 811.531 nm.

Diagnosis theory

Local velocity and temperature measurements are based on Doppler shift, v_D and Doppler half-width of an absorption line, Δv_0 , respectively. The Doppler shift is strategically determined by simultaneous recording of absorption profiles of two laser beams having a different incident angle to the flow. Although a perpendicular and an oblique laser beams are usually chosen in velocity measurements, a transmission beam through an argon discharge tube was used in this experiment to get the relative zero point of Doppler shift to simplify the test. The flow velocity can be derived from the relative shift of the absorption peak frequencies between the transmissions through the argon discharge tube and the argon plasma flow.

$$V = (v_D c) / (v_0 \cos \phi) \quad (1)$$

Temperature of the gas can be determined from the broadening feature of the absorption line. The shape of line broadening would be the Voigt profile containing Lorentz broadening and Doppler broadening. Since Doppler broadening is the predominant broadening mechanism in the case with high temperature and low pressure flows,^{3,7)} the absorption line shape can be simplified as the following function;

$$g_D(v) = \frac{2}{\Delta v_0} \sqrt{\frac{\ln 2}{\pi}} \exp\left(-4 \ln 2 \frac{(v - v_0)^2}{\Delta v_0^2}\right) \quad (2)$$

where the correlation between the temperature and the Doppler half width is

$$\Delta v_0 = \frac{2v_0}{c} \sqrt{\frac{2 \ln 2 kT}{m}} \quad (3)$$

With the knowledge of the Ar I absorption wavelength of 811.531 nm and the laser incident angle of 60 degrees, the

Doppler shift is directly related to the velocity by the following relation

$$V = 1623.0 v_D \text{ (GHz)} \quad (4)$$

The temperature is expressed as

$$T = 570.91 [\Delta v_0 \text{ (GHz)}]^2 \quad (5)$$

In order to determine the number density of the absorbing particles, absolute value of the absorption coefficient, κ_0 is required;

$$N = \frac{\Delta v_0}{2} \sqrt{\frac{\pi}{\ln 2}} \frac{mc \kappa_0}{\pi e^2 f} \quad (6)$$

κ_0 is available from the spatial differentiation of the absorption, $I_0 - I_{\phi}$, because it is an integration of absorption coefficient along the laser path. Practically, the computer tomography method is often used to have a three-dimensional absorption coefficient distribution.

Computer tomography method

Two-dimensional ($r-x$) distribution of the absorption coefficient are obtained without a rotational scanning of laser beams assuming axisymmetric plume configuration. The laser beam is introduced into the vacuum chamber through an optical fiber. The fiber, a collimating lens and a detector are attached to the stage mounted on a two-dimensional traverse system as shown in Fig. 3.

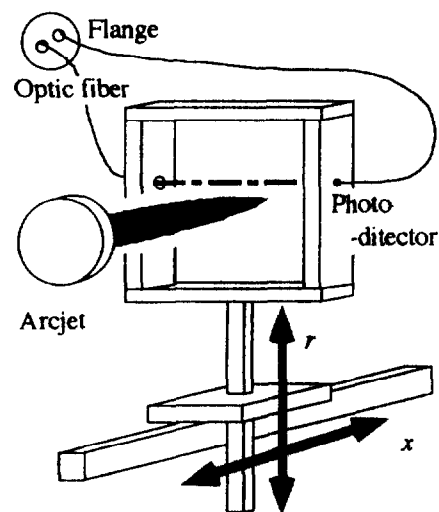


Fig. 3 Optic arrangement mounted on a two-dimensional traverse system.

The filtered back-projection method with Sheppard-Logan filter function is used for the data processing. The data-processing procedure is shown in Fig. 4.

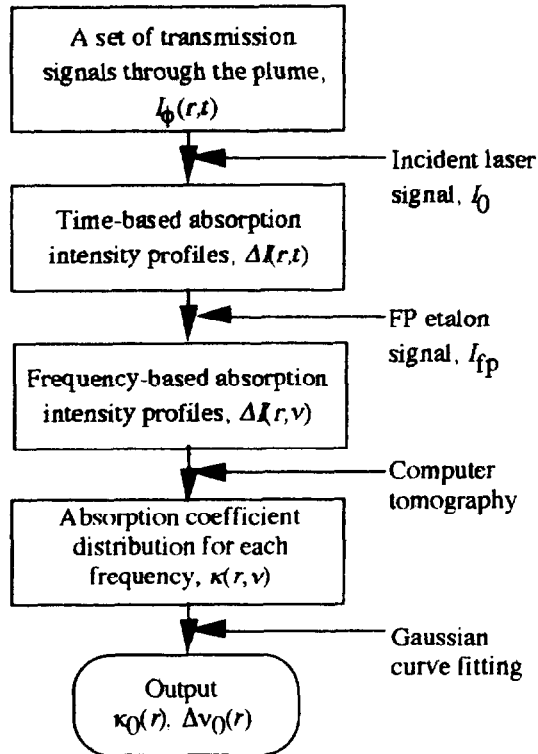


Fig. 4 Data-processing procedure flow-chart

Results and discussions

Doppler measurements

A total of sixty cases of measurements is performed at the propellant flow rate ranging from 0.06 g/s to 0.3 g/s and the discharge current from 100 A to 180 A. Figure 5 shows the typical record of the detector signals.

Each recorded trace consists of 10,030 datapoints at an interval about 0.02 μ sec. The FP etalon transmission signal contains 40 fringes as seen in Fig. 5 (b). Because of the nonsymmetric characteristic of the diodelaser, the peak position of the FP etalon fringes is not equidistant in time in ascending and descending ramps. The recorded absorption signal is converted from the time based one to the frequency based one by the comparison of frequency spacing with FP etalon fringes. A three parameter Gaussian line-shape fitting was conducted on the absorption profiles to determine peak frequencies and the Doppler half width. Deduced profiles are shown in Fig. 6.

The flow velocities and temperatures are derived from v_D and Δv_0 using Eqs. (4) and (5), respectively. Figure 7 show the correlation of plume velocity and specific input power for various propellant flow rate measured at 7.0 cm downstream of the nozzle exit plane. Higher velocity is marked with the larger propellant flow rate. This is

interpreted as a phenomenon that the anode heat loss is decreased with the increase in propellant flow rate. (It has been reported that the anode temperature is decreased with the increase in propellant flow rate.^{10,11)})

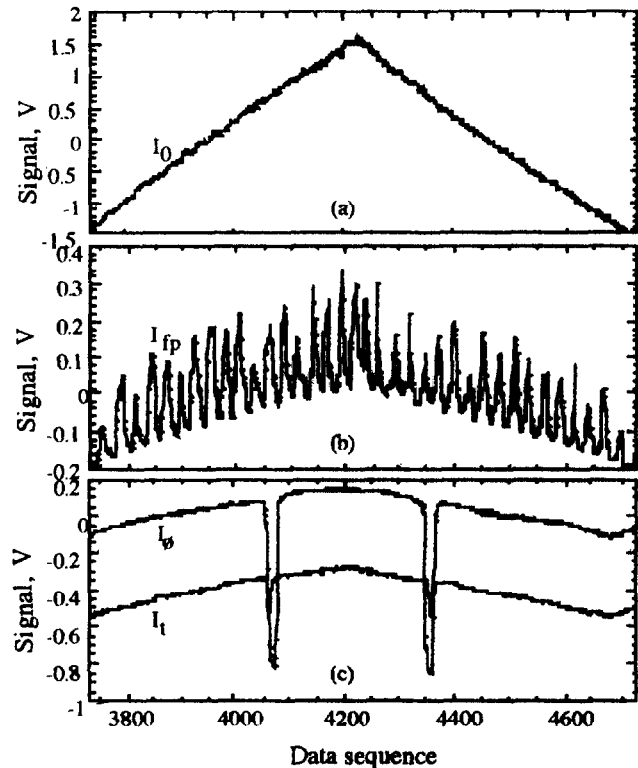


Fig. 5 Typical records. (a) temporal variation of incident laser intensity. (b) Fabry-Perot etalon signal, (c) transmission profile of the oblique probe laser beam (upper) and the one through the argon discharge tube (lower).

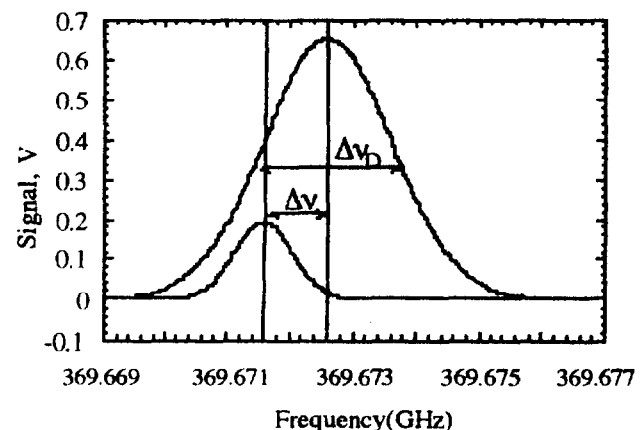


Fig. 6 Absorption profile of the transmitted lasers through the arcjet plume (upper) and the argon discharge tube (lower).

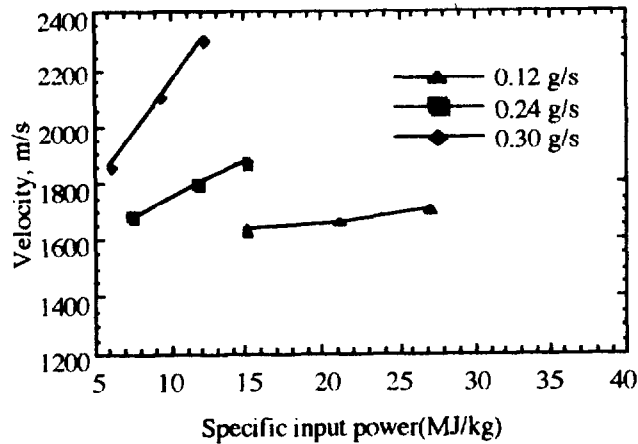


Fig. 7 Plume velocity vs. specific input power measured at 7.0 cm downstream of the nozzle exit plane.

At a low propellant flow rate, the velocity increase becomes quite small. This would be because the background gas causes a relatively large momentum transfer with the plume plasma, as described later.

Comparison of the measured local velocity at $x = 7$ cm with the mean flow velocity derived from thrust measurements was shown in Fig. 8. Its increasing trend with the specific input power is agree with the mean velocity one.

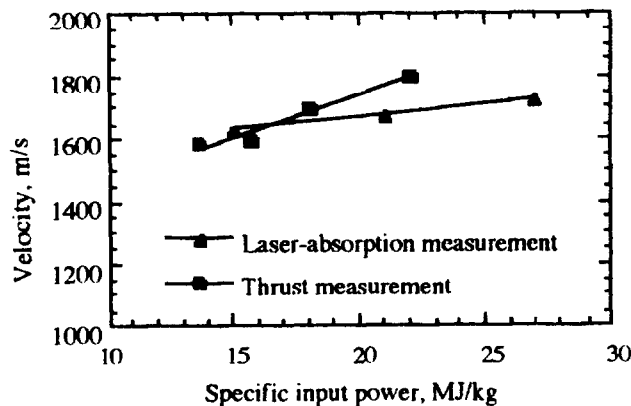


Fig. 8 Measured local velocity with the mean flow velocity derived from thrust measurements. Propellant mass flow rate is 0.12 g/s.

Distributions of velocity and temperature along the thruster centerline are shown in Figs. 9 and 10, respectively. Both of them are decreased quickly near the nozzle exit plane. This indicates that the arcjet plume experiences a large momentum and energy transfer to the entrained background gas near the exit plane.⁴⁾

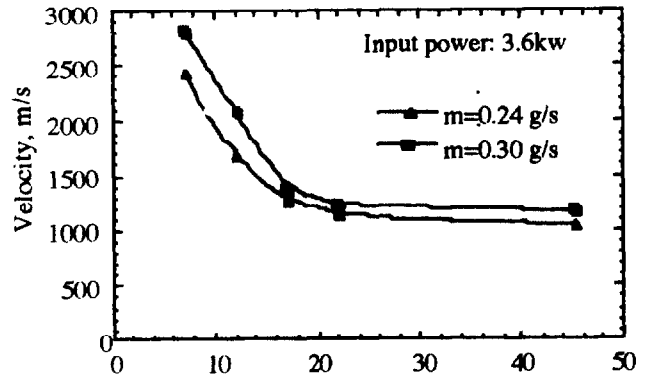


Fig. 9 Distributions of the velocity along the thruster centerline.

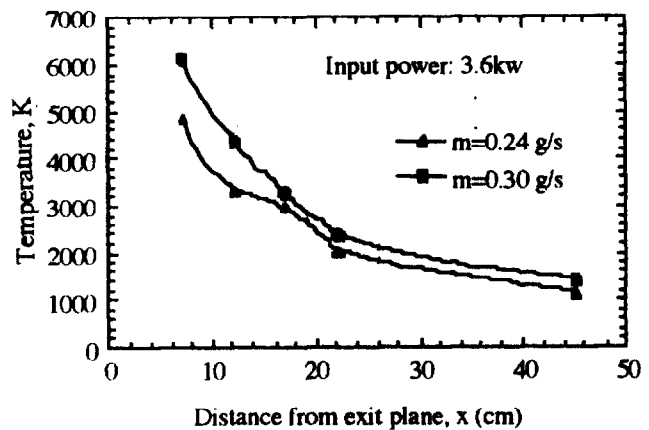


Fig. 10 Distributions of the temperature along the thruster centerline.

Computer tomography measurement

Figures 11 and 12 show the plume temperature and density contours. The spatial resolution was $\Delta r = 6$ mm in the radial direction and $\Delta x = 50$ mm in the axial direction. The maximum temperature and density were 10,000 K and $1.5 \times 10^{18} \text{ m}^{-3}$, respectively.

Swirl velocity measurement

Swirl velocity caused by the Lorenz force was measured with a probe laser perpendicular to the plume. Applying the magnetic field, discharge voltage was increased by 2~3 volts, which is about 10 % of the discharge voltage. The measured velocity was 194 ± 157 m/s at $r = 11$ mm and $x = 9$ mm under the conditions of magnetic induction 800 gauss, discharge current 180 A and propellant flow rate 0.24 g/s. This value is too small to cause an efficient swirl acceleration.

From a simple kinetic model, the swirl velocity can be

expressed as a function of the arc-length, which is the distance from the centerline to the arc attachment position on the diverging part of anode, as;

$$V_{\text{swirl}} = (BI/m) (r_{\text{arc}}^2/r) \quad (7)$$

The swirl velocity of 194 m/s corresponds to the arc-length of 6.0 mm according to this equation.

Large swirl velocity will be obtained with the hydrogen propellant because the arc tends to blow out toward the edge of anode when molecular gas is used as a propellant, resulting in long arc-length.¹²⁾

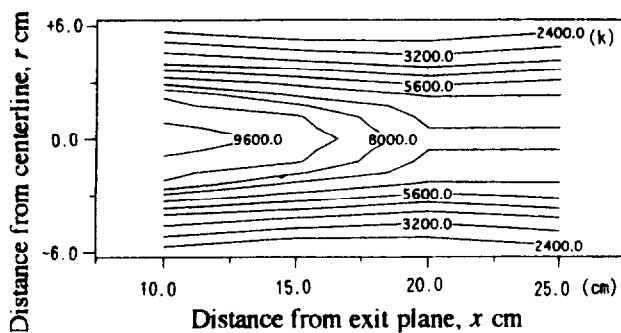


Fig. 11 Two-dimensional distribution of the translational temperature of the argon neutral atoms. Input power 1.8 kW, propellant flow rate 0.24 g/s.

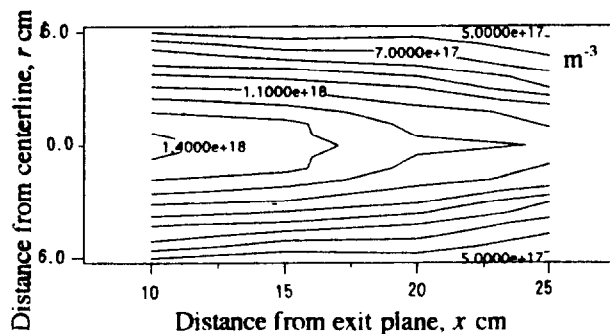


Fig. 12 Two-dimensional distribution of the number density of the argon neutral atoms. Input power 1.8 kW, propellant flow rate 0.24 g/s.

References

1. Tahara, H., Uda, N., Tsubakishita, Y. and Yoshikawa, T., "Optical measurement and numerical

analysis of medium-power arcjet non-equilibrium flowfields, Proc. of 23rd Int'l Electric Propulsion Conf., IEPC 93-133, Seattle, WA, September, 1993.

2. Gulczynski, F.S., King, L.B., Foster, J.E., Kim, S.W., and Gallimore, A.D.: Near and Far-field Plume Studies of a 1 kW Arcjet, 30th Joint propulsion conf., AIAA Paper 94-2743, Indianapolis, IN, 1994.

3. Liebeskind, J. G., Hanson, R. K. and Cappelli, M. A., "Laser-Induced Fluorescence Diagnostics for Temperature and Velocity Measurements in a Hydrogen Arcjet Plume," Appl. Opt. 32, pp. 6117- 6127 (1993).

4. Storm, P. V. and Cappelli, M. A., "Axial Emission Measurement on a Medium Power Hydrogen Arcjet Thruster," AIAA paper 94-3137, 1994.

5. Philippe, L. C. and Hanson, R. K., "Laser Diode Wave-Length Modulation spectroscopy for Simultaneous Measurement of Temperature, Pressure and Velocity in Shock-Heated Oxygen Flows," Appl. Opt. 20, pp. 6090-6103 (1993).

6. Arroyo, M. P., Langlois, S., and Hanson, R. K., "Diode-Laser Absorption Technique for Simultaneous Measurements of Multiple Gas-dynamic Parameters in High-Speed Flows Containing Water Vapor," Appl. Opt. 33, pp. 3296-3307 (1994).

7. Luck, K.C., Thielen, W.: Measurement of Temperatures and OH-Concentrations in a lean Methane-Air Flame Using High-Resolution Laser-Absorption Spectroscopy, J. Quantum Spectroscopy and Radiation Transfer. Vol. 20, pp. 71-79.

8. Miller, P. : Tunable Diode Laser Measurement of Carbon Monoxide Concentration and Temperature in a Laminar Methane-Air Diffusion Flame, Appl. Opt., 32 (913), pp. 6082-6089.

9. Rea, E.C. and Hanson, R.K.: Rapid Extendedrange tuning of single mode ring dye lasers, Appl. Opt., 22 (1983), pp. 518-520.

10. Yoshikawa, T., Onoe, K., Tsuru, S., Ishii, M. and Uematsu, K., : Development of a low power Arcjet Thruster, Proc. of 22nd Int'l Electric Propulsion Conf., IEPC 91-012, Viareggio, Italy, 1991.

11. Sankovic, J.M., Hamley, J.A., Haag, T.W.: Hydrogen Arcjet Technology, Proc. of 22nd Int'l Electric Propulsion Conf., IEPC 91-012, Viareggio, Italy, 1991.

12. Tahara, H., Kagaya, Y., Yoshikawa, T.: Effects of Applied Magnetic Fields on Performance of a Quasisteady Magnetplasmadynamic Arcjet, J. Propulsion and power, Vol.11, No. 2, pp. 337-342